

# A Bis(diazadiene) Adduct of MoCl<sub>2</sub>: Mononuclear, Octahedral, Undistorted and Diamagnetic

François Stoffelbach,<sup>[a]</sup> Bertrand Rebière,<sup>[a]</sup> and Rinaldo Poli\*<sup>[a,b]</sup>

**Keywords:** Density functional calculations / Magnetic properties / Molybdenum / N ligands / X-ray diffraction

The complex [MoCl<sub>2</sub>(*i*Pr<sub>2</sub>dad)<sub>2</sub>] (*i*Pr<sub>2</sub>dad = *i*PrN=CH=CH=N-*i*Pr) is obtained in one step by reduction of [MoCl<sub>3</sub>(THF)<sub>3</sub>] in the presence of *i*Pr<sub>2</sub>dad. The X-ray structure reveals a relatively undistorted octahedral coordination geometry with a relative *cis* configuration and points to a more appropriate description of the ligands as enediamides. The NMR investigation is in agreement with the same *cis* structure in solution and underlines the diamagnetism of the compound, at odds with previously reported very similar complexes. A bulk

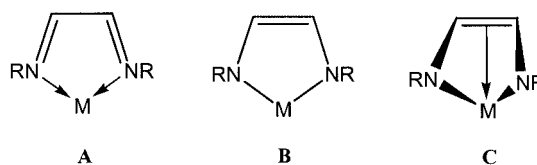
magnetic susceptibility measurement further confirms the compound's diamagnetism. No equilibrium with a dinuclear, metal-metal bonded species is apparent from the solution studies. A DFT calculation on the real molecule and on two R<sub>2</sub>dad model systems with R = Ph and 4-HOC<sub>6</sub>H<sub>4</sub> reveals how the ligand periphery delicately controls the magnetic and structural properties of this system.

(© Wiley-VCH Verlag GmbH & Co. KGaA, 69451 Weinheim, Germany, 2004)

## Introduction

The coordination chemistry of diazadiene ligands (RN=CH=CH=NR; R<sub>2</sub>dad) has attracted attention for quite some time,<sup>[1,2]</sup> because their high electronic and coordination mode flexibility (i.e. see **A**, **B** and **C**) imparts unusual electron-donor and -acceptor properties to these ligands, combining the useful features of N-based donors such as bipy and unsaturated acceptors such as dienes. Consequently, these ligands are generally compatible with metal centers in both high and low oxidation states. For some time, we have been investigating the coordination chemistry and the organometallic chemistry of molybdenum in intermediate oxidation states, mostly II, III and IV. Ligands with mild  $\pi$ -acidic properties, such as phosphanes, are quite compatible with these systems, but a wide range of ligands with extreme  $\sigma$ - and  $\pi$ -donor/acceptor properties also afford isolable and stable compounds. It was therefore of interest to probe the coordination of diazadiene ligands to these ions. We have recently shown<sup>[3]</sup> that a variety of R<sub>2</sub>dad ligands easily add to [CpMoCl<sub>2</sub>] to yield [CpMoCl<sub>2</sub>(R<sub>2</sub>dad)] complexes and a crystallographic study indicates that the dad ligand adopts a coordination mode closest to **B**. The metal center, therefore, is most appropriately described as formally Mo<sup>V</sup>. In this contribution, we report the synthesis, the structural and physical characteriz-

ation, and a DFT study of a compound resulting from the formal addition of two *i*Pr<sub>2</sub>dad ligands to MoCl<sub>2</sub>. The product presents several unusual features when compared with other compounds that are very closely related to it.



## Results and Discussion

The complex [MoCl<sub>2</sub>(*i*Pr<sub>2</sub>dad)<sub>2</sub>] (*i*Pr<sub>2</sub>dad = *i*PrN=CH=CH=N-*i*Pr) was prepared in one step from [MoCl<sub>3</sub>(THF)<sub>3</sub>] by reduction with Zn in the presence of the diazadiene ligand. A similar strategy was previously used for the preparation of the related R<sub>2</sub>dad complex with R = C<sub>6</sub>H<sub>4</sub>OMe-4,<sup>[4]</sup> and for the preparation of related [MoCl<sub>2</sub>(R<sub>2</sub>dad)(CNMe)<sub>2</sub>] complexes when conducted in the presence of methyl isocyanide, the main difference being the use of sodium as the reducing agent.<sup>[5]</sup> These other derivatives of MoCl<sub>2</sub>, however, were not structurally characterized and no details of their stereochemistry (e.g. *cis* vs. *trans*) were evident from the spectroscopic studies.

The NMR properties unambiguously establish the diamagnetic nature of the compound and establish the *cis* stereochemistry of the molecule in solution. In fact, the four isopropyl methyl groups of an individual dad ligand are all inequivalent, as expected for the C<sub>2</sub> molecular symmetry, whereas they would all be equivalent for the C<sub>2v</sub>-symmetric

<sup>[a]</sup> Laboratoire de Synthèse et d'Electrosynthèse Organométalliques, Faculté des Sciences "Gabriel", Université de Bourgogne, 6 Boulevard Gabriel, 21000 Dijon, France

<sup>[b]</sup> Laboratoire de Chimie de Coordination 205 Route de Narbonne, 31077 Toulouse Cedex, France Fax: (internat.) + 33-5-61553003 E-mail: poli@lcc-toulouse.fr

trans isomer. Since the two dad ligands are symmetry related, four methyl peaks are observed overall in the <sup>1</sup>H NMR spectrum, each being split to a doublet by coupling with the corresponding methyne proton. The methyne protons correspondingly give rise to two different septets and the inner CH=N protons to two mutually coupled signals with a very small coupling constant (2.0 Hz).

Crystals of the [MoCl<sub>2</sub>(*i*Pr<sub>2</sub>dad)<sub>2</sub>] derivative suitable for an X-ray structural study could be grown from diethyl ether at low temperature. The structural analysis confirms the identity of the molecule and establishes the *cis* stereochemistry (see Figure 1). The geometry is essentially regular octahedral, the only slight deviations being attributable to the small bite of the chelating dad ligands [N(1)–Mo–N(2) = 75.55(8)° and N(3)–Mo–N(4) = 75.52(8)°]. The N(1) and N(3) ligands are essentially perfectly opposite to each other [N(1)–Mo–N(3) = 177.93(8)°] and at nearly right angles to both Cl atoms.

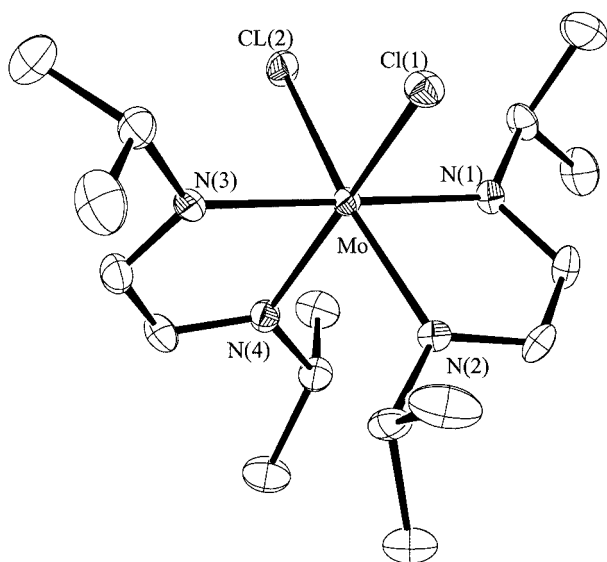


Figure 1. An ORTEP view of the geometry of [MoCl<sub>2</sub>(*i*Pr<sub>2</sub>dad)<sub>2</sub>]

The Mo–dad five-membered rings are essentially planar [RMS deviation of fitted atoms = 0.0433 and 0.0256 for the MoN(1)C(1)C(2)N(2) and MoN(3)C(9)C(10)N(4) cycles, respectively; highest deviations from the plane: 0.0553(14) Å for atom N(2) and 0.0329(14) Å for atom N(3)]. The N–C distances average 1.338(8) Å and the C–C distances average 1.372(4) Å. These are considerably lengthened and shortened, respectively, when compared with those of free dad molecules such as *s-trans*-Cy<sub>2</sub>dad [N–C: 1.258(2) Å; C–C: 1.457(2) Å] and also with those of complexes to which the bonding mode A can be clearly assigned (N–C: 1.26–1.30 Å; C–C: 1.40–1.46 Å).<sup>[1]</sup> The observed structural parameters are more consistent with a bonding description where the arrangement B plays a significant role and are very similar to those of our recently reported dad adduct of [CpMoCl<sub>2</sub>].<sup>[3]</sup> Compounds such as the formally d<sup>6</sup> [Mo(CO)<sub>4</sub>(R<sub>2</sub>dad)] (R = *i*Pr or C<sub>6</sub>H<sub>3</sub>-*i*Pr<sub>2</sub>-2,6),<sup>[6]</sup> d<sup>4</sup>

[Mo(allyl)Br(CO)<sub>2</sub>(R<sub>2</sub>dad)] (R = *t*Bu, Ph),<sup>[7,8]</sup> and d<sup>0</sup> [MoO<sub>2</sub>Cl<sub>2</sub>(*t*Bu<sub>2</sub>dad)],<sup>[9]</sup> on the other hand, show N–C and C–C parameters much closer to those of the free dad ligands, in better agreement with coordination mode A. Other Mo complexes with dad or dad-related ligands are also known.<sup>[10–13]</sup> We can advance the hypothesis that the dad ligand cannot operate as an effective π-acid in the above mentioned d<sup>6</sup> and d<sup>4</sup> complexes because of the competition with the stronger carbonyl ligands.

The Mo–N distances are slightly longer for the N(1) and N(3) atoms that are trans to each other, than for the N(2) and N(4) atoms located trans to the Cl atoms, reflecting the greater trans influence of the imino donors. The Mo–N distances are considerably shorter than in the structurally related complex [MoO<sub>2</sub>Cl<sub>2</sub>(*t*Bu<sub>2</sub>dad)] [2.399(2) and 2.388(2) Å], where the two oxo ligands satisfy the maximum valence of the molybdenum center and therefore the dad ligand can only bind via the coordination mode A.<sup>[9]</sup> This is further supporting evidence for the description of the coordination geometry as B in the title compound. The Mo–Cl distances average 2.404(1) Å, these also being shorter than those found in other *cis*-dichloro complexes of Mo<sup>II</sup> with strong *trans* ligands, for example 2.52(1) Å in [MoCl<sub>2</sub>(dppe)<sub>2</sub>],<sup>[14]</sup> and closer to typical Mo<sup>VI</sup>–Cl distances, such as 2.356(1) Å in [MoO<sub>2</sub>Cl<sub>2</sub>(*t*Bu<sub>2</sub>dad)]<sup>[9]</sup> and 2.3251(7) Å in [(C<sub>5</sub>H<sub>7</sub>Pr<sub>4</sub>)MoO<sub>2</sub>Cl],<sup>[15]</sup> in further agreement with the assignment of a higher formal oxidation state to the metal in compound 3.

The compound's diamagnetism is the most surprising result concerning this compound, especially when compared with the paramagnetism (two unpaired electrons) measured for the very similar [MoCl<sub>2</sub>(R<sub>2</sub>dad)<sub>2</sub>] and [MoCl<sub>2</sub>(R<sub>2</sub>dad)(CNMe)<sub>2</sub>] (R = C<sub>6</sub>H<sub>4</sub>-OMe-4) complexes<sup>[4,5]</sup> and which is reasonably expected for low-spin octahedral d<sup>4</sup> Mo<sup>II</sup> complexes, an example of which is [MoCl<sub>2</sub>(PMe<sub>3</sub>)<sub>4</sub>].<sup>[16]</sup> Related W<sup>II</sup> complexes with the same dad ligand are also paramagnetic.<sup>[4]</sup> The bulk diamagnetism of the title compound was confirmed by a magnetic susceptibility study. The striking difference between the two [MoCl<sub>2</sub>(R<sub>2</sub>dad)<sub>2</sub>] compounds (diamagnetic for R = *i*Pr, paramagnetic for R = C<sub>6</sub>H<sub>4</sub>-OMe-4), under the assumption that the aryl derivative has a similar structure, leads to the hypothesis that the *i*Pr-substituted ligand is a better π-acceptor, delocalizing the metal electrons onto the ligand more effectively by adopting a binding mode closer to type B (as verified by the X-ray structural analysis), whereas the *p*-MeO-phenyl-substituted ligand leads to a molecule where the ligand adopts a binding mode closer to type A and which can be described more appropriately as a coordination compound of Mo<sup>II</sup>. It seems rather surprising, however, that the 4-MeOC<sub>6</sub>H<sub>4</sub> substitution would render the dad ligand a poorer π-acceptor than substitution by *i*Pr. This question has been addressed in more detail by a DFT investigation (see below).

Another peculiar feature of the title compound, given its diamagnetism, is the fact that no *major* distortion is revealed by the X-ray structural analysis. In fact, the large family of diamagnetic octahedral complexes of Mo<sup>II</sup> (d<sup>4</sup>) typically show rather severe distortions from the ideal octa-

hedral geometry, with angles between bonds in relative cis positions as low as 72° and as high as 120°.<sup>[17]</sup> In the title compound, on the other hand, the only evident structural deformation is a straightforward consequence of the small bite of the two dad ligands. This phenomenon can again be rationalized on the basis of the extensive back-bonding to the dad ligands which is revealed by the solid-state structural data, so that the compound can no longer be assimilated as an octahedral d<sup>4</sup> dichlorobis(dad) complex of Mo<sup>II</sup>. An electrochemical investigation of the title compound in THF shows two reversible one-electron processes, a reduction at  $E_{1/2} = -1.27$  V and an oxidation at  $E_{1/2} = -0.24$  V (Figure 2). Evidently, the orbitals involved in the electron addition and removal processes are more or less delocalized between the metal center and the ligands.

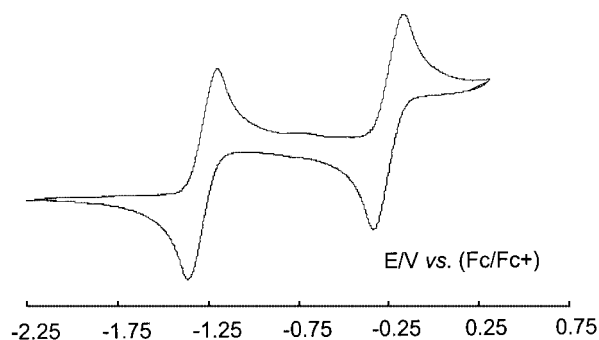


Figure 2. Cyclic voltammogram of a THF solution of [MoCl<sub>2</sub>(iPr<sub>2</sub>dad)<sub>2</sub>]

In order to explore the details of the electronic structure for this compound and to understand the effect of the peripheral groups on the dad coordination mode, we have carried out DFT calculations on three different [MoCl<sub>2</sub>(R<sub>2</sub>dad)<sub>2</sub>] systems with R = *i*Pr (the “real” system), Ph and 4-HOC<sub>6</sub>H<sub>4</sub>. The pairwise comparison between these three systems allows us to assess the electronic effect of aryl vs. alkyl groups on the dad ligand, as well as the effect of a para substituent with a mesomeric donating effect on the aryl groups. The computationally simpler OH substituent was used instead of the OMe substituent which is present in the literature compound,<sup>[4]</sup> since we only wish to probe the electronic effect of the OR conjugation with the aryl group. No major steric effect is expected to differentiate the electronic action of the *p*-OH and OMe groups.

All three systems have been fully optimized in both singlet and triplet states. The relative energies of the two spin states are reported in Table 1 together with relevant optimized geometrical parameters. First, it can be noted that the DFT-optimized structure for the real molecule in the spin singlet compares very closely with the experimentally determined structure (cf. first column of Table 1 with the data in Table 2). In particular, the C–N and C–C distances for the dad ligand are in close agreement with the experimental structure and with a description where the enediamido form **B** plays a significant role, whereas the triplet molecule

Table 1. DFT optimized bond lengths [Å] and angles [deg], and relative energies in kcal mol<sup>−1</sup>, for compounds MoCl<sub>2</sub>(R<sub>2</sub>dad)<sub>2</sub>

	R = <i>i</i> Pr		R = Ph		R = 4-HOC <sub>6</sub> H <sub>4</sub>	
	Singlet	Triplet	Singlet	Triplet	Singlet	Triplet
Mo–Cl	2.495	2.522	2.461	2.498	2.467	2.507
Mo–N( <i>t</i> )	2.097	2.146	2.098	2.159	2.101	2.161
Mo–N( <i>c</i> )	2.060	2.111	2.082	2.146	2.081	2.146
N–C	1.356	1.337	1.361	1.343	1.361	1.344
C–C	1.396	1.422	1.392	1.416	1.391	1.415
Cl–Mo–Cl	105.54	92.51	111.24	93.84	110.12	93.57
N–Mo–N (chel)	75.70	75.45	75.30	75.38	75.40	75.51
N–Mo–N ( <i>cis</i> )	83.97	95.05	81.16	84.20	81.18	84.01
N–Mo–N ( <i>trans</i> )	173.84	168.42	173.39	169.23	174.45	168.64
E	0.00	2.85	0.00	2.09	0.00	−4.40

Table 2. Bond lengths [Å] and angles [deg] for [MoCl<sub>2</sub>(iPr<sub>2</sub>dad)<sub>2</sub>]

Bond length	Bond length
Mo–N(1) 2.082(2)	Mo–N(2) 2.046(2)
Mo–N(3) 2.072(2)	Mo–N(4) 2.038(2)
Mo–Cl(1) 2.4046(7)	Mo–Cl(2) 2.4027(6)
N(1)–C(1) 1.338(3)	N(1)–C(6) 1.493(3)
N(2)–C(2) 1.326(3)	N(2)–C(3) 1.488(3)
N(3)–C(9) 1.345(3)	N(3)–C(14) 1.495(3)
N(4)–C(10) 1.342(3)	N(4)–C(11) 1.486(3)
C(1)–C(2) 1.369(4)	C(9)–C(10) 1.375(4)
Bond angle	Bond angle
N(1)–Mo–N(2) 75.55(8)	N(2)–Mo–N(3) 106.02(8)
N(1)–Mo–N(3) 177.93(8)	N(2)–Mo–N(4) 83.41(8)
N(1)–Mo–N(4) 103.43(8)	N(3)–Mo–N(4) 75.52(8)
N(1)–Mo–Cl(1) 91.66(6)	N(3)–Mo–Cl(1) 89.80(7)
N(1)–Mo–Cl(2) 89.23(6)	N(3)–Mo–Cl(2) 89.03(6)
N(2)–Mo–Cl(1) 87.07(6)	N(4)–Mo–Cl(1) 159.47(6)
N(2)–Mo–Cl(2) 162.47(6)	N(4)–Mo–Cl(2) 91.96(6)
Cl(2)–Mo–Cl(1) 102.22(2)	

shows longer C–N and shorter C–C distances, in agreement with reduced Mo–dad back-bonding. The angular parameters are not dramatically different in the two spin states. The opposite Cl–Mo–Cl and N–Mo–N(*cis*) angles become closer to the ideal octahedral values in the triplet state, whereas the N–Mo–N(*trans*) angle is less distorted in the singlet state. The optimized molecules with R = Ph and 4-HOC<sub>6</sub>H<sub>4</sub> have geometrical features in close proximity to the R = *i*Pr system for both spin states.

The most interesting feature is the effect of R on the relative energy. For R = *i*Pr and Ph, the singlet state is more stable than the triplet by approximately the same amount (2–3 kcal mol<sup>−1</sup>). Therefore, a change from an alkyl to an aryl group does not affect very much the electronic structure at the metal center. On the other hand, the addition of an OH substituent in the para position of the aryl group inverts the stability order in favor of the triplet state, in

perfect agreement with the experimental results reported by Pombeiro et al.<sup>[4]</sup> We have attempted to pinpoint the reason for this unexpected result by inspecting the orbital interactions that are responsible for the Mo-dad bonding. As it turns out, the observed trend results from the combination of minor energy changes caused by the *p*-OH group on several bonding molecular orbitals in the deep energy region. From a qualitative point of view, we can argue that the *p*-OMe group, through its  $\pi$ -donating effect, makes the aryl group less capable of accepting electron density from the dad system and consequently renders the dad ligand a poorer  $\pi$ -acceptor, the ultimate effect being a relative destabilization of the singlet state. Some support for this statement comes from an analysis of the Mulliken charges (see Table 3). In the singlet state, the metal atom has a lower positive charge in the order 4-HOC<sub>6</sub>H<sub>4</sub> < Ph < *i*Pr and, significantly, the HOC<sub>6</sub>H<sub>4</sub> group has a greater positive charge relative to Ph.

Table 3. Mulliken charges for compounds [MoCl<sub>2</sub>(R<sub>2</sub>dad)<sub>2</sub>]

	R = <i>i</i> Pr		R = Ph		R = 4-HOC <sub>6</sub> H <sub>4</sub>	
	Singlet	Triplet	Singlet	Triplet	Singlet	Triplet
Mo	0.706	0.668	0.681	0.727	0.668	0.671
N (total)	-1.343	-1.255	-1.619	-1.683	-1.602	-1.496
R (total)	0.719	0.783	1.026	1.042	1.058	1.077

The energies of the relevant frontier orbitals for the three calculated systems in both spin states are shown in Figure 3. The shape of the five orbitals for the singlet *i*Pr system, i.e. the title compound, are also shown. It can be seen that the overall trend of the MO energies is identical in all three cases, in particular on going from the Ph to the 4-HOC<sub>6</sub>H<sub>4</sub> substituent. The Mo-dad back-bonding interaction is present with an approximately identical intensity in the HOMO and in the second highest occupied MO (SHOMO), as revealed by the contribution from the N atomic orbitals. For the SHOMO, this is quite evident from the contour plot included in Figure 3, whereas the HOMO maximizes its interaction with the dad ligand on the opposite side of the molecule (not visible). The LUMO is essentially a pure metal orbital, whereas the two higher energy empty orbitals are slightly Mo-dad antibonding ( $\pi^*$ ). The three lowest orbitals (SHOMO, HOMO and LUMO) also exhibit a small contribution from the Cl atoms which is Mo–Cl  $\pi^*$  in nature.

The two Mo-dad  $\pi$ -interactions are responsible for the large splitting of the pseudo-octahedral “*t*<sub>2g</sub>” set of orbitals and for the consequent adoption by the molecule of the singlet spin-state. It is to be noted that one of these two Mo-dad  $\pi$  bonding orbitals remains doubly occupied also in the triplet configuration, whereas one electron from the other orbital becomes Mo-dad nonbonding in the triplet state. Therefore, the overall Mo-dad  $\pi$  back-bonding interaction is only slightly reduced upon going from the singlet to the triplet. The MO analysis also shows that, in spite of the Mo-dad  $\pi$ -interaction, the major contribution to the

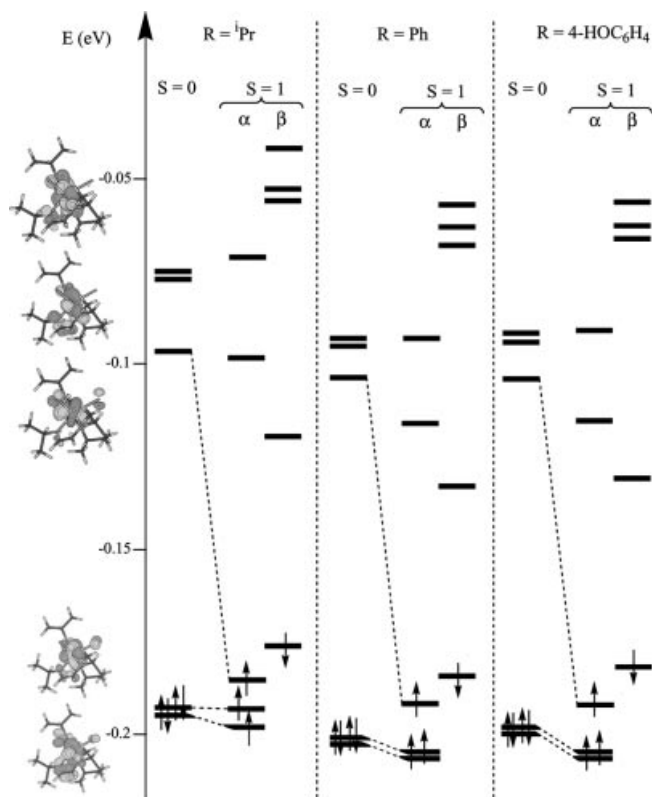


Figure 3. Energy diagram of the five 4d-derived frontier orbitals for singlet and triplet [MoCl<sub>2</sub>(R<sub>2</sub>dad)<sub>2</sub>] (R = *i*Pr, Ph, and 4-HOC<sub>6</sub>H<sub>4</sub>); on the left, MOLDEN views of the five orbitals for the singlet R = *i*Pr compound are also shown

HOMO remains that of the Mo atomic orbitals, while the Mulliken analysis shows that the majority of the spin density is localized on the Mo atom. Therefore, the one-electron oxidation process that is observed in the cyclic voltammetric study may be considered to be essentially a metal-based process. This observation serves to illustrate, once again, that the attribution of formal oxidation states has only a limited bookkeeping value when the ligands are able to adapt to their electronic environment via tunable  $\pi$ -interactions. This problem is commonplace in organometallic chemistry, for instance for M-olefin, M-diene, M-carbene complexes, and so forth.<sup>[18]</sup> The title compound may be described by the two limiting forms as a bis(diazadiene) Mo<sup>II</sup> complex (bonding of type A), or as a bis(enediamido) Mo<sup>VI</sup> complex (bonding of type B), or as anything in between. The real situation can only be revealed by the experimental observations (structural parameters, redox potentials, and so forth) and interpreted on the basis of the MO calculations.

A final interesting observation concerns the absence of any dinuclear product of formula [Mo<sub>2</sub>Cl<sub>4</sub>(dad)<sub>2</sub>], containing a quadruple Mo–Mo bond. There are numerous examples of [Mo<sub>2</sub>Cl<sub>4</sub>L<sub>4</sub>] compounds where the neutral ligands are N-based donors, mostly saturated amines,<sup>[19–24]</sup> but also nitriles,<sup>[25]</sup> pyridines,<sup>[26,27]</sup> bipyridines and other aromatic amines.<sup>[28]</sup> This observation may once again be rationalized by considering the strong  $\pi$ -accepting properties



of the dad ligand. It is known, in fact, that strongly  $\pi$ -acidic ligands disfavor metal-metal bonds<sup>[29,30]</sup> and favor the establishment of mononuclear structures.

## Conclusions

Compound  $[\text{MoCl}_2(i\text{Pr}_2\text{dad})_2]$  is a remarkable coordination compound because of its diamagnetism, at odds with very similar complexes. The X-ray structure shows a relatively undistorted mononuclear octahedral coordination geometry for the complex, with bond lengths that are in better agreement with a bis(enediamido)  $\text{Mo}^{\text{VI}}$  model than with a bis(diazadiene)  $\text{Mo}^{\text{II}}$  model. The greater propensity of the di-*i*Pr-substituted dad ligand to adopt an enediamido coordination relative to the bis( $\text{C}_6\text{H}_4\text{OMe-4}$ )-substituted dad ligands was not anticipated. The theoretical investigation shows the propensity of the dad ligands to accept electron density from the metal center in the HOMO and SHOMO and to reorganize to a coordination mode closer to that of enediamido ligands. These orbitals, however, retain a substantial metal contribution.

## Experimental Section

**General procedures:** All manipulations were carried out under an atmosphere of dry and oxygen-free argon with standard Schlenk techniques. Toluene and diethyl ether were purified by reflux over sodium benzophenone ketyl and distilled under argon prior to use. The cyclic voltammogram was obtained with an EG&G 362 potentiostat connected to a Macintosh computer through MacLab hardware/software. The electrochemical cell was fitted with a Ag-AgCl reference electrode, a platinum disk working electrode and a platinum wire counter electrode.  $[\text{Bu}_4\text{N}]\text{PF}_6$  (ca. 0.1 M) was used as supporting electrolyte in THF. All potentials are reported relative to ferrocene standard, which was added to the solution at the end of the experiment and measured at 100 mV/s.  $[\text{MoCl}_3(\text{THF})_3]$ <sup>[31]</sup> and the *i*Pr<sub>2</sub>dad ligand<sup>[32]</sup> were prepared as described in the literature. The elemental analyses were carried out by the analytical service of the laboratory with a Fisons EA 1108 apparatus. NMR spectra were recorded in  $\text{C}_6\text{D}_6$  at 25 °C on a Bruker DRX 500 spectrometer. The peaks positions are reported with positive shifts in ppm downfield of TMS, as calculated from residual solvent peaks.

**Synthesis of  $[\text{MoCl}_2(i\text{Pr}_2\text{dad})_2]$ :**  $[\text{MoCl}_3(\text{THF})_3]$  (1.25 g, 2.99 mmol), Zn (0.2 g, 3.05 mmol) and *i*Pr<sub>2</sub>dad (0.903 g, 6.44 mmol) were suspended in 15 mL of toluene at room temperature. The mixture was then stirred for three days at room temperature. The solution was filtered through Celite to remove an insoluble residue, evaporated to dryness, and warmed to 70 °C under vacuum in order to sublime the residual *i*Pr<sub>2</sub>dad. A crude product was obtained as a red dark microcrystalline solid. Yield: 0.92 g (69.2%). Recrystallization by cooling from  $\text{Et}_2\text{O}$  at –80 °C afforded X-ray quality crystals, one of which was used for the X-ray structural study.  $\text{C}_{16}\text{H}_{32}\text{Cl}_2\text{MoN}_4$  (447.3): calcd. C 42.96, H 7.21, N 12.53; found C 43.19, H 7.30, N 12.21. Cyclic voltammetry (THF): reversible oxidation at  $E_{1/2} = -0.24$  V ( $\Delta E_p = 185$  mV) and reversible reduction at  $E_{1/2} = -1.27$  V ( $\Delta E_p = 177$  mV) (the ferrocene peak shows  $\Delta E_p = 248$  mV). IR data (Golden gate):  $\tilde{\nu} = 2968$   $\text{cm}^{-1}$ , 2926m, 2867m, 1490s, 1457m, 1363m, 1229s, 1219s, 1172s,

1121m, 1097m, 1024m, 795s.  $^1\text{H}$  NMR ( $\text{C}_6\text{D}_6$ , 25 °C):  $\delta = 0.32$  (d,  $J = 6.6$  Hz,  $\text{CH}_3$ ), 0.47 (d,  $J = 6.7$  Hz,  $\text{CH}_3$ ), 1.12 (d,  $J = 6.7$  Hz,  $\text{CH}_3$ ), 1.54 (d,  $J = 6.6$  Hz,  $\text{CH}_3$ ), 4.18 (sept,  $J = 6.6$  Hz, CH), 5.15 (sept,  $J = 6.7$  Hz, CH), 6.02 (d,  $J = 2.0$  Hz,  $\text{CH}=\text{N}$ ), 6.52 (d,  $J = 2.0$  Hz,  $\text{CH}=\text{N}$ ) ppm.  $\chi_M = -143.2 \times 10^{-6}$  cgs units (calculated correction for the ligand diamagnetism:  $\chi_M = -259.6 \times 10^{-6}$  cgs units).

**X-ray Analysis of  $[\text{MoCl}_2(i\text{Pr}_2\text{dad})_2]$ :** Intensity data were collected on a Nonius–Kappa CCD at 110 K. The structure was solved via a Patterson search program<sup>[33]</sup> and refined with full-matrix least-squares methods based on  $F^2$  (SHELXL-97)<sup>[33]</sup> with the aid of the WINGX program.<sup>[34]</sup> All non-hydrogen atoms were refined with anisotropic thermal parameters. H atoms were found in a difference Fourier map and refined freely with their isotropic displacement parameters fixed at 1.2 or 1.5 (for  $\text{CH}_3$ ) times the  $U_{\text{eq}}$  of their parent atoms. Refinement of the Flack parameter<sup>[35]</sup> showed that the crystal is an inversion twin<sup>[36]</sup> with a twin fraction of 0.54(3). The crystal data and refinement parameters are collected in Table 4, whereas selected bond lengths and angles are listed in Table 2.

Table 4. Crystal data and structure refinement for  $[\text{MoCl}_2(i\text{Pr}_2\text{dad})_2]$

Formula	$\text{C}_{16}\text{H}_{32}\text{Cl}_2\text{MoN}_4$
Mol. mass	447.30
$T$ (K)	110(2)
Crystal system	orthorhombic
Space group	$P2_12_12_1$
$a$ (Å)	9.5125(2)
$b$ (Å)	11.9721(2)
$c$ (Å)	18.9856(4)
$V$ (Å <sup>3</sup> )	2162.17(7)
$Z$	4
$F(000)$	928
$D_{\text{calc}}$ (g/cm <sup>3</sup> )	1.374
Diffractionmeter	Enraf–Nonius KappaCCD
Scan type	mixture of $\phi$ rotations and $\omega$ scans
$\lambda$ (Å)	0.71073
$\mu$ (mm <sup>–1</sup> )	0.858
Crystal size (mm <sup>3</sup> )	$0.3 \times 0.175 \times 0.125$
$\sin(\theta)/\lambda$ max (Å <sup>–1</sup> )	0.65
Index ranges	$h$ : –10; 12 $k$ : –15; 15 $l$ : –24; 21
Absorption correction	SCALEPACK
RC = Refl. Collected	12354
IRC = independent RC	4861 [ $R(\text{int}) = 0.0343$ ]
IRCGT = IRC and $[I > 2\sigma(I)]$	4380
Refinement method	full-matrix least-squares on $F^2$
Data/restraints/parameters	4861/0/305
$R$ for IRCGT	$R1^{[a]} = 0.0290$ , $wR2^{[b]} = 0.0497$
$R$ for IRC	$R1^{[a]} = 0.0367$ , $wR2^{[b]} = 0.0520$
Goodness-of-fit <sup>[c]</sup>	1.013
Absolute structure parameter	0.54(3)
Largest diff. peak and hole (e <sup>–</sup> Å <sup>–3</sup> )	0.544 and –0.692

<sup>[a]</sup>  $R1 = \Sigma(|F_o| - |F_c|)/\Sigma|F_o|$ . <sup>[b]</sup>  $wR2 = [\Sigma w(F_o^2 - F_c^2)^2]/\Sigma[w(F_o^2)^2]^{1/2}$  where  $w = 1/[\sigma^2(F_o^2) + 0.00 \cdot P + (0.0212 \cdot P)^2]$  and  $P = [\text{Max}(F_o^2, 0) + 2 \cdot F_c^2]/3$ . <sup>[c]</sup> Goodness of fit =  $[\Sigma w(F_o^2 - F_c^2)^2/(N_o - N_c)]^{1/2}$ .

CCDC-206713 contains the supplementary crystallographic data for this paper. These data can be obtained free of charge at [www.ccdc.cam.ac.uk/conts/retrieving.html](http://www.ccdc.cam.ac.uk/conts/retrieving.html) [or from the Cambridge

Crystallographic Data Centre, 12 Union Road, Cambridge CB2 1EZ, UK; Fax: (internat.) +44-1223/336-033; E-mail: deposit@ccdc.cam.ac.uk].

**Computational Details:** All calculations were performed using the Gaussian 98 program package.<sup>[37]</sup> The three-parameter form of the Becke, Lee, Yang and Parr functional (B3LYP),<sup>[38]</sup> was employed, in combination with the LanL2DZ library of basis functions, which includes both Dunning and Hay's D95 sets for H, C, O and N<sup>[39]</sup> and the relativistic Electron Core Potential (ECP) sets of Hay and Wadt for the 10 inner electrons of Cl and the 28 inner electrons of Mo.<sup>[40–42]</sup> All geometries were fully optimized without symmetry restrictions. For the open-shell species, the calculations used unrestricted open-shell methods. The mean value of the spin over the electronic density in an unrestricted calculations does not reproduce exactly the assigned spin multiplicity. In all our cases, though, it was considered to be suitable to identify unambiguously the spin state. Mean values of  $\langle S^2 \rangle$  were in the narrow 2.097–2.174 range for triplets. In all cases, relative energies are given in kcal mol<sup>−1</sup> and do not include a correction for zero-point energy.

## Acknowledgments

We thank the CNRS and the French Ministry of Research for funding and Dr. P. Richard for assistance. F. S. thanks the CNRS and the Conseil Régional de Bourgogne for a BDI fellowship.

- [1] G. Van Koten, K. Vrieze, *Adv. Organomet. Chem.* **1982**, *21*, 151–239.
- [2] K. Vrieze, *J. Organomet. Chem.* **1986**, *300*, 307–326.
- [3] F. Stoffelbach, R. Poli, P. Richard, *J. Organomet. Chem.* **2002**, *663*, 269–276.
- [4] A. J. L. Pombeiro, M. F. N. N. Carvalho, *Rev. Port. Quim.* **1981**, *23*, 23–32.
- [5] A. J. L. Pombeiro, R. L. Richards, *Transition Met. Chem.* **1981**, *6*, 255–258.
- [6] H. tom Dieck, T. Mack, K. Peters, H. G. Vonschnering, *Z. Naturforsch., Teil B* **1983**, *38*, 568–579.
- [7] A. J. Graham, D. Akridge, B. Sheldrick, *Acta Crystallogr., Sect. C* **1983**, *39*, 192–194.
- [8] A. J. Graham, D. Akridge, B. Sheldrick, *Acta Crystallogr., Sect. C* **1985**, *41*, 995–996.
- [9] K. Dreisch, C. Andersson, C. Stalhandske, *Polyhedron* **1993**, *12*, 303–311.
- [10] R. Beckert, M. Doring, H. Gorls, F. Knoch, E. Uhlig, J. Wuckelt, *J. Prakt. Chem.* **1995**, *337*, 38–42.
- [11] C. Kapplinger, R. Beckert, W. Imhof, *J. Prakt. Chem.* **1998**, *340*, 323–333.
- [12] M. Doring, H. Gorls, R. Beckert, *Z. Anorg. Allg. Chem.* **1994**, *620*, 551–560.
- [13] M. G. B. Drew, V. Félix, I. S. Gonçalves, F. E. Kühn, A. D. Lopes, C. C. Romão, *Polyhedron* **1998**, *17*, 1091–1102.
- [14] G. Pelizzi, G. Predieri, *Gazz. Chim. Ital.* **1982**, *112*, 381–386.
- [15] D. Saurens, F. Demirhan, P. Richard, R. Poli, H. Sitzmann, *Eur. J. Inorg. Chem.* **2002**, 1415–1424.
- [16] E. Carmona, J. M. Marín, M. L. Poveda, J. L. Atwood, R. D. Rogers, *Polyhedron* **1983**, *2*, 185–193.
- [17] P. Kubáček, R. Hoffmann, *J. Am. Chem. Soc.* **1981**, *103*, 4320–4332.
- [18] J. P. Collman, L. S. Hegedus, J. R. Norton, R. G. Finke, *Principles and Applications of Organotransition Metal Chemistry*, University Science Books, **1987**.
- [19] F. A. Cotton, E. V. Dikarev, S. Herrero, *Inorg. Chem.* **1998**, *37*, 5862–5868.
- [20] F. A. Cotton, E. V. Dikarev, S. Herrero, *Inorg. Chem.* **1999**, *38*, 490–495.
- [21] F. A. Cotton, E. V. Dikarev, S. Herrero, *Inorg. Chem.* **1999**, *38*, 2649–2654.
- [22] F. A. Cotton, E. V. Dikarev, S. Herrero, *Inorg. Chem.* **2000**, *39*, 609–616.
- [23] M. Gerards, *Inorg. Chim. Acta* **1995**, *229*, 101–103.
- [24] H. L. Chen, C. T. Lee, C. T. Chen, J. D. Chen, L. S. Liou, J. C. Wang, *J. Chem. Soc., Dalton Trans.* **1998**, 31–35.
- [25] F. A. Cotton, R. Poli, *J. Am. Chem. Soc.* **1988**, *110*, 830–841.
- [26] F. A. Cotton, E. V. Dikarev, S. Herrero, B. Modéc, *Inorg. Chem.* **1999**, *38*, 4882–4887.
- [27] F. A. Cotton, E. V. Dikarev, J. D. Gu, S. Herrero, B. Modéc, *J. Am. Chem. Soc.* **1999**, *121*, 11758–11761.
- [28] D. M. Baird, F. L. Yang, D. J. Kavanaugh, G. Finness, K. R. Dunbar, *Polyhedron* **1996**, *15*, 2597–2606.
- [29] P. Brant, F. A. Cotton, J. C. Sekutowski, T. E. Wood, R. A. Walton, *J. Am. Chem. Soc.* **1979**, *101*, 6588–6593.
- [30] F. A. Cotton, D. J. Darensbourg, B. W. S. Kolthammer, *J. Organomet. Chem.* **1981**, *217*, C14–C16.
- [31] F. Stoffelbach, D. Saurens, R. Poli, *Eur. J. Inorg. Chem.* **2001**, 2699–2703.
- [32] J. M. Kligman, R. K. Barnes, *Tetrahedron Lett.* **1969**, *24*, 1953–1956.
- [33] G. M. Sheldrick, 'SHELX97 (Includes SHELXS-97 and SHELXL-97), Release 97–2, Programs for Crystal Structure Analysis', University of Göttingen, **1998**.
- [34] L. J. Farrugia, *J. Appl. Crystallogr.* **1999**, *32*, 837–838.
- [35] H. D. Flack, *Acta Crystallogr., Sect. A* **1983**, *39*, 876–881.
- [36] H. D. Flack, G. Bernardinelli, *Acta Crystallogr., Sect. A* **1999**, *55*, 908–915.
- [37] M. J. Frisch, G. W. Trucks, H. B. Schlegel, G. E. Scuseria, M. A. Robb, J. R. Cheeseman, V. G. Zakrzewski, J. Montgomery, J. A., R. E. Stratmann, J. C. Burant, S. Dapprich, J. M. Millam, A. D. Daniels, K. N. Kudin, M. C. Strain, O. Farkas, J. Tomasi, V. Barone, M. Cossi, R. Cammi, B. Mennucci, C. Pomelli, C. Adamo, S. Clifford, J. Ochterski, G. A. Petersson, P. Y. Ayala, Q. Cui, K. Morokuma, D. K. Malick, A. D. Rabuck, K. Raghavachari, J. B. Foresman, J. Cioslowski, J. V. Ortiz, A. G. Baboul, B. B. Stefanov, G. Liu, A. Liashenko, P. Piskorz, I. Komaromi, R. Gomperts, R. L. Martin, D. J. Fox, T. Keith, M. A. Al-Laham, C. Y. Peng, A. Nanayakkara, C. Gonzalez, M. Challacombe, P. M. W. Gill, B. Johnson, W. Chen, M. W. Wong, J. L. Andres, C. Gonzalez, M. Head-Gordon, E. S. Replogle, J. A. Pople, Gaussian 98, Revision A.9, Gaussian, Inc., **1998**.
- [38] A. D. Becke, *J. Chem. Phys.* **1993**, *98*, 5648–5652.
- [39] T. H. Dunning, Jr., P. J. Hay, *Modern Theoretical Chemistry* (Ed. H. F. Schaefer, III), Plenum, New York, **1976**.
- [40] P. J. Hay, W. R. Wadt, *J. Chem. Phys.* **1985**, *82*, 270–283.
- [41] W. R. Wadt, P. J. Hay, *J. Chem. Phys.* **1985**, *82*, 284–298.
- [42] P. J. Hay, W. R. Wadt, *J. Chem. Phys.* **1985**, *82*, 299–310.

Received March 28, 2003

Early View Article

Published Online January 2, 2004